1
Fe, Ru, and Os Nanoparticles

Madhu Kaushik, Yuting Feng, Nathaniel Boyce, and Audrey Moores

1.1
Introduction

Although Fe, Ru, and Os are transition metals all belonging to Group 8 of the periodic table, their prevalence, chemistry, and applications differ greatly. Iron is an earth abundant element, playing a key role in life with implications in some of the most difficult biological processes [1]. Iron is a current topic of interest in the context of catalysis, both in its homogeneous [2, 3] and heterogeneous forms [4, 5], as a means to replace more toxic and less abundant transition metals. Iron has interesting properties in this context, including magnetic properties, a rich redox chemistry, with implications both in molecular and material sciences, an affordable price and nontoxicity. Iron complexes, oxides, and metal-based materials have been applied to a wide array of chemical processes, including oxidation processes, hydrogenation, C–C coupling, and aromatic substitutions [3, 6–9]. Ruthenium belongs to the platinum series and is obtained as a by-product to platinum or nickel mining. Within the platinum series, ruthenium is comparably cheaper than its counterparts and thus desirable as a replacement to more expensive, catalytically active transition metals. Compared to iron, it is less prone to oxidation when in its reduced form. Ruthenium has established itself as an important and industrially relevant catalyst, in both its homogeneous and heterogeneous forms for a number of important processes including the Haber-Bosch process (dinitrogen to ammonia) [10, 11], the Fischer-Tropsch process (syngas to hydrocarbons) [12, 13], hydrogenation reactions [14], including the partial and selective hydrogenation of benzene and phenol, olefin metathesis [15], CH activation [16], and organic oxidations just to name a few. Osmium has been comparatively less explored. Osmium tetroxide and related compounds have demonstrated early on their ability to catalyze the oxidative cleavage of olefins with molecular oxygen [17]. Other osmium complexes have now been developed for a number of reactions including complete and partial hydrogenation, dehydrogenation, and hydroformylation [18, 19]. Nanoparticulate osmium counterparts

Nanocatalysis in Ionic Liquids, First Edition. Edited by Martin H.G. Prechtl.

have been studied for their catalytic properties toward Fischer–Tropsch reaction, the homologation of alkenes under H_2 and the hydrogenolysis of alkanes [20], and electrocatalytic activity useful in fuel cell research [21].

Ionic liquids (ILs) are defined as salts with melting points below 100 °C. Over the last two decades, research on ILs has developed with a focus on liquid ones at or near room temperature [22, 23]. Typically such systems are constituted of flexible organic ion pairs with delocalized charges and tunable lipophilic domains [24]. Because of their liquid nature and specific properties, ILs are used as solvents to substitute volatile molecular liquids and specialty materials for a number of important applications, including synthesis, catalysis and biocatalysis, separation technology, biomass processing and transformation, electrochemical devices including capacitors, fuel cells and solar cells, nanotechnology, sensing, lubricants, hypergolic materials, and pharmaceutics [22, 25–30]. ILs rapidly emerged as a privileged environment for catalysis because of their unique intrinsic properties. ILs are attractive as potential solvents for a number of reasons: (i) they are nonvolatile under ambient conditions; (ii) they are colorless and little viscous; (iii) they possess good solvation properties for a large number of species; (iv) they are immiscible with many conventional solvents; (v) The properties of ILs can be easily tuned by a careful choice of the cation and anion entities, making them "designer solvents" [31]; and (vi) they are commercially available [30]. The combination of properties (i), (iii), (iv), and (v) explain that they are perfectly suited as catalyst stabilizers in biphasic systems [32, 33]. ILs have also been developed in supported versions to afford heterogenized systems of interest in catalysis [27].

Metal nanoparticles (NPs) have been intensely researched in the context of catalysis [34, 35]. Their high surface-over-volume ratio and unique effects linked to their nano size (role of defects, photon, and electron-linked properties) explain unique activities at the crossroads of homogeneous and heterogeneous catalysis [36–38]. They are appealing as highly active catalysts and materials easily amenable to recovery and recycling strategies [37]. Metal NPs and ILs, as privileged catalysts and catalysis media respectively, have thus been naturally explored in partnership and have opened a unique and rich research field, which has already been largely reviewed. Among the papers published over the last 10 years, the reader is directed to reviews on ILs in catalysis [25, 39], functionalized ionic liquids (FILs) [40, 41], FILs in catalysis [42], NPs in ILs [36, 43–46], NPs in ILs for catalysis [26, 47–55], and Ru NPs in IL [56]. In this chapter, we focused on the synthesis, stabilization properties, and catalytic applications of Fe, Ru, and Os NPs in ILs. For Fe, we extended the review to iron oxide NPs as well, as under aerobic condition, reduced iron NPs lead to such species.

1.2 Synthesis of Fe, Ru, and Os NPs in ILs

In general, the synthetic methods to access metal and metal oxide NPs in ILs have focused on providing materials with key features relevant for catalysis,

that is, small sizes, good monodispersity, and high purity [26]. These properties are achieved using bottom-up synthetic approaches, either by reduction of metal salts, by the direct use of zero-valent molecular species, which can be freed from their ligands via hydrogenation, or simply decomposed (Scheme 1.1). The use of additional stabilizers [46] or functional ILs [42] has been reported to improve the properties of the end product. Top-down approaches are known for the synthesis of Au, Rh, Pd, and Pt NPs in ILs but are not a classic approach to access NPs of metals of Group 8 [26]. Also, although synthetic routes via phase transfer [57] from another organic or aqueous medium have been reported for other metals such as gold [58] and rhodium [59], Group 8 NPs are typically prepared directly in neat ILs. Because of the preorganized structure of ILs via electrostatic, hydrogen bonding, and van der Waals interactions, especially those with imidazolium and phosphonium functionalities, the IL medium is described as made of polar and nonpolar nanodomains. Those tunable domains act as nanoreactors and stabilizing chambers via noncovalent interactions [44, 46]. Thanks to the polarity, thermal stability, and preorganized supermolecular structure of ILs, the synthesis of Ru, Fe, and Os NPs could be attained in ambient conditions [44, 60]. In ILs, such strategies have unlocked access to metal NPs with precise size control and narrow size distributions [56]. Further comments on the stabilization properties of ILs for NPs are provided in Section 1.3.

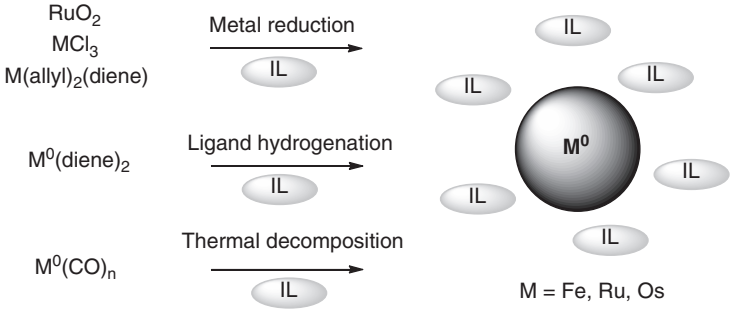

Scheme 1.1 Summary of the synthetic schemes for accessing Fe, Ru, and Os NPs in ILs.

A complete list of Ru NPs synthesis in ILs was established by Campbell *et al.* in 2013 [56]. In the following sections, we focused on the most distinctive and recent examples for synthesis of Fe, Ru, and Os NPs. One of the specifics of the synthesis of metal NPs directly within an IL is the difficulty in washing the resulting material from any salt by-product generated during the reaction. Hence it is important to select "salt-free" precursors or organometallic precursors decomposing into easily washable organic species or volatile [61, 62] ones, such as [Ru(COD)(2-methylallyl)$_2$], [Ru(COD)(COT)], or carbonyl compounds such as (COD = 1,5-cyclooctadiene and COT = 1,3,5-cyclooctatriene) [63], as discussed below.

1.2.1
Synthesis via Reduction of Metal Precursors or Ligands

Despite the long list of reducers used with this metal, Ru precursors in ILs are reduced by H_2 in reported procedures [36, 48, 56, 64]. In a common scheme, a Ru precursor, such as [Ru(COD)(2-methylallyl)$_2$] or [Ru(COD)(COT)] is dissolved or suspended into a specific IL under argon and exposed to mild H_2 pressure and heating (<90 °C) from a few hours to days to obtain a black suspension. The size of the resulting Ru NPs – usually between 1.0 and 3.0 nm – and their size distribution may be tuned depending on reaction conditions, namely, stirring, temperature, and IL cations/anions (Figure 1.1) [56, 65–70]. From a formal standpoint, [Ru(COD)(2-methylallyl)$_2$] and [Ru(COD)(COT)] precursors differ in that the latter is a Ru(0) complex which should not necessitate the use of a reducer. Under H_2 pressure, however, the COD and COT ligands are hydrogenated to release atomic Ru(0) and allow the growth of Ru NPs [61, 62]. $RuCl_3$ and RuO_2 have also been reported as precursors being easily reduced by H_2 to access the desired NPs. In some ILs, precursor solubility may be a limitation that has been circumvented via the use of an auxiliary solvent. Our group showed that tetrahydrofuran (THF) could be successfully used to mix [Ru(COD)(2-methylallyl)$_2$] with phosphonium and imidazolium ILs, before being easily removed *in vacuo*. Subsequent reduction under H_2 pressure afforded small Ru NPs (between 1.5 and 2.5 nm) [71]. Although not necessarily required for subsequent catalytic applications, the separation of the obtained NPs from imidazolium ILs may be performed and depends on the anion in the IL [65]. Prechtl *et al*. also showed that

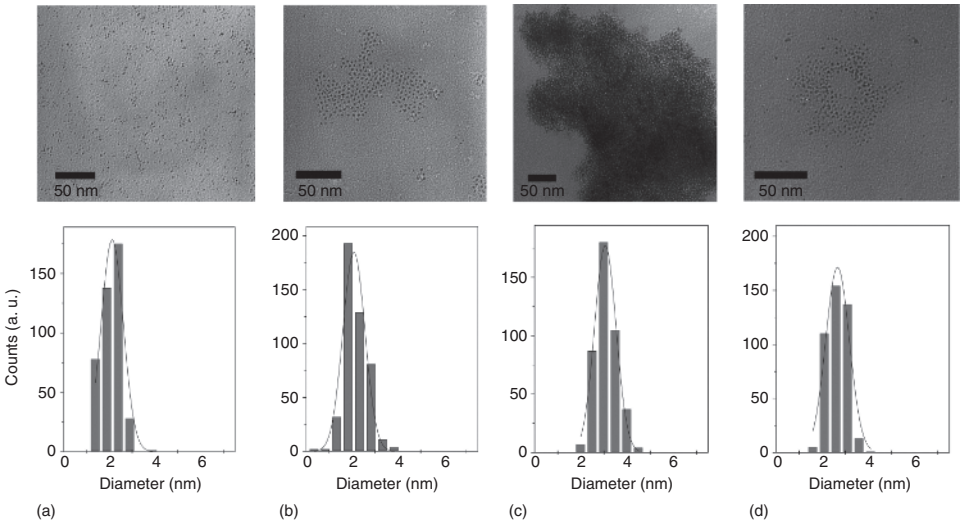

Figure 1.1 *In situ* transmission electron microscopy (TEM) images of Ru NPs generated from the reduction of [Ru(COD)(2-methylallyl)$_2$] by H_2 in (a) [C_4C_1Im][NTf_2], (b) [$C_{10}C_1$Im][NTf_2], (c) [C_4C_1Im][BF_4], and (d) [$C_{10}C_1$Im][BF_4]. (Prechtl *et al.* [65]. Reproduced with the permission of American Chemical Society.)

imidazolium ILs containing NTf_2 (bis(trifluoromethylsulfonyl)imide) anions such as $[C_4Im][NTf_2]$ and $[C_6C_1Im][NTf_2]$ could be used directly as reducing agents toward $[Ru(COD)(2\text{-methylallyl})_2]$ [72]. Small and monodisperse 2.0 ± 0.3 nm Ru NPs were obtained at low temperature and atmospheric pressure without the participation of classical reducing agents such as H_2, $LiAlH_4$, or hydrazine. The $^-NTf_2$ anion was shown to have a key role in the reduction mechanism; imidazolium ring decomposition was also observed.

On the other hand, the use of Grignard reagents with $FeCl_3$ successfully afforded catalytically active Fe(0) NPs of 4–5 nm diameter [73].

Upon intensive use in catalysis or through simple aging, IL-stabilized NPs have been shown to grow, coalesce, or leach. A study by Scott and coworkers showed that tetraalkylphosphonium ILs were a good environment to produce metal NPs of Au, Pd, Pt, Ru, Rh, Ni, Co, Fe, Ag, and Cu from halide salts, using appropriate reducers, for example, $LiBH_4$ for Ru and Fe [74]. These NPs could be oxidized back into salts in the presence of oxygen for oxidizable metals such as Fe or *tert*-butyl hydroperoxide for Ru. Further addition of reducer allowed recovery of the metal NPs within the IL.

1.2.2
Synthesis via Decomposition of Metal Precursors

The decomposition of metal complexes in IL involves various energy forms such as heat, microwave, and light irradiation [46]. The Thomann and Janiak groups [75] reported successful synthesis of Fe, Ru, and Os NPs by the decomposition of their respective di- and trinuclear metal carbonyls in *n*-butyl-methylimidazolium tetrafluoroborate $[C_4C_1Im][BF_4]$. Under argon, the deoxygenized dry IL with dissolved or suspended metal carbonyl was heated to 250 °C for several hours; alternatively, the mixture was irradiated with UV light at 200–450 nm for 15 min. The products are in the range of several nanometers and with a uniform, monodisperse, and narrow size distribution. By varying the metal loading, the NP size could be varied as well. For Fe, Fe(0) and Fe_2O_3 NPs were produced under inert and aerobic conditions respectively, with sizes of 5.2 ± 1.6 and 4.2 ± 1.1 nm, respectively. For Ru and Os, the sizes achieved were smaller, between 1.6 ± 0.4 and 2.0 ± 0.5 nm for Ru and 2.5 ± 0.4 nm for Os. Under inert atmosphere, the products could be retained for months. This procedure was updated later so that the reaction is finished in 3 min (for 0.48 g IL in a 1 ml vial) by microwave irradiation (10 W) [76]. The same group also synthesized chemically derived graphene (CDG)-supported Ru NPs from $Ru_3(CO)_{12}$ in $[C_4C_1Im][BF_4]$ [77]. $Ru_3(CO)_{12}$ was added into preformed CDG/IL slurry (0.2 wt%) and stirred for 18 h under argon. The whole mixture then went through a 6-min microwave irradiation (20 W). The dried flakes after centrifugation and decantation were analyzed and proved to be Ru NPs attached to mini CDG sheets (Ru NP/CDG) with 17.4 wt% Ru content. In another example, Lee *et al.* synthesized Fe_2O_3 nanobars and nanowires in $[C_8C_1Im][BF_4]$/dimethylformamide mixture by thermal decomposition of $Fe(CO)_5$ followed by oxidation [78]. The IL $[C_8C_1Im][BF_4]$

played an important role in stabilizing NPs, directing crystal growth to obtain high aspect ratio particles as well as boosting thermal decomposition of the precursor. The resulting high aspect ratio NPs showed good superparamagnetic properties, useful for contrast enhancement applications.

1.2.3 The Use of Additional Stabilizers and Functional ILs

ILs are privileged media used to generate and maintain small metal NPs useful in catalysis. However, upon using and reusing IL-stabilized metal NPs, it has been noted that the NPs could aggregate and lose their catalytic activity [55]. Also, for specialty applications, highly monodisperse metal NPs may be needed, which are difficult to achieve with straight IL. To overcome these hurdles, additional stabilizers have been used, either in the form of small molecules [46] or in the form of FILs [40–42]. In the context of NP stabilization, *FILs* are defined as an IL featuring a metal-binding moiety such as a phosphine, an amine, or a thiol. A few examples of such strategies have been reported with Fe and Ru metals. Highly monodispersed, iron oxide NPs of 10.6 ± 1.6 nm were made in 1-butyl-3-methylimidazolium bis(triflylmethyl-sulfonyl) imide ($[C_4C_1Im][NTf_2]$) by thermal decomposition of $Fe(CO)_5$ in the presence of oleic acid as an additional stabilizer, followed by oxidation (Figure 1.2a) [79]. The control over the particle size was attributed to the oversaturation of oleic acid in the system.

The resulting particles could be allowed to settle and be separated from the IL, which was recycled and reused for another synthesis. In this example, Fourier-transform infrared (FTIR) spectroscopy was used to establish that the oleic acid alone was responsible for the NP stabilization. The size of these iron oxide NPs could be tuned by using a mixture of stabilizers composed of oleic acid, oleylamine, and 1,2-hexadecanediol [79]. Using a similar procedure, the same group synthesized iron oxide NPs in $[C_4C_1Im][NTf_2]$ with different

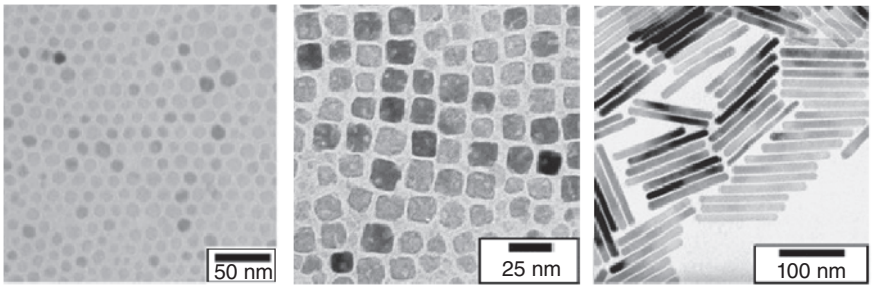

Figure 1.2 TEM images of iron oxide (a) nanospheres, (b) nanocubes, and (c) nanorods synthesized in $[C_4C_1Im][NTf_2]$ by thermal decomposition of $Fe(CO)_5$ using oleic acid and/oleylamine as capping agent. (Panel (a) Wang *et al*. [79]. Reproduced with the permission of Royal Society of Chemistry. Panels (b) and (c) Wang and Yang [80]. Reproduced with the permission of Elsevier.)

morphologies, such as nanorods and nanocubes, by playing on the reaction temperature, the nature of the stabilizer (oleic acid and oleylamine), as well as the concentration of these stabilizers (Figures 1.2b and c) [80].

Besides small molecules, FILs were also shown to provide improved stabilization compared to classic ILs. A few examples of Group 8 NPs produced in FILs were recently reported. With Ru, phosphine-functionalized imidazolium-based ILs were used as stabilizers to access catalytically active 2.2 nm Ru NPs [81]. Nitrile [82] and hydroxy [83]-functionalized imidazolium IL were also used to access Ru NPs, which proved particularly appealing as selective catalysts for partial hydrogenation of nitriles, hydrogenation of C=O, and hydrogenation of C=C bonds. Interestingly, the 1-butyronitrile-3-methylimidazolium bis(trifluoromethanesulfonyl)imidate IL ($[(C_3CN)C_1Im][NTf_2]$) afforded small Ru NPs (2.2 ± 0.5 nm), comparable to the ones obtained in nonfunctionalized ILs, while 1-(2,3-dihydroxypropyl)-2,3-dimethylimidazolium bis(trifluoromethanesulfonimide) $[C_1C_1(EG)Im][NTf_2]$ gave larger NPs (6.9 ± 1.3 nm) [82, 83]. With Fe, polymer-based ILs, namely, an imidazolium-modified poly(ethylene glycol) was used as the medium to access ferrite NPs. The resulting system functioned as a ferrofluid and served as electrolyte in an AC circuit [84]. Jacobi von Wangelin and coworkers reported the synthesis of Fe(0) NPs stabilized with nitrile-functionalized imidazolium generated within an imidazolium-based IL. This system was used for the selective hydrogenation of alkynes into alkene, as further detailed in Section 1.4.2 [73].

1.3
Ionic Liquid Stabilization of Metal Nanoparticles

1.3.1
Ionic Liquid Properties

Metal NPs are intrinsically unstable materials that easily grow into bulk metal by particle coalescence. In the liquid phase, they thus require the use of stabilizers in the form of small molecules or polymeric materials to ensure that they remain stable as a suspension. ILs are quite unique in this context, as they provide an environment that has the intrinsic ability to stabilize NPs extensively without the use of a stabilizer. ILs have thus been termed "nanosynthetic templates" [75, 85]. The origin of this stabilization has been studied using a number of techniques and remains an active area of research with open questions and debates. The structure of free, pure ILs is complex and has been explored using experimental and theoretical approaches [22]. Neutron scattering experiments have allowed to establish that structural order in imidazolium-based ILs extends over a longer range than conventional liquids, although this effect is dependent upon the nature of the counter anion [86–88]. ILs also differ from convention solvents in that they feature mesoscopic organizations. The surfactant properties of ILs originating from the presence of hydrophilic and hydrophobic functionalities translate in the liquid phase into the presence of polar and nonpolar mesodomains.

1.3.2
Molecular Aspects of Ionic Liquid Stabilization of Metal Nanoparticles

The presence of nanodomains is of prime importance when studying the interaction of ILs with metal NPs, especially the smaller ones (1–3 nm), because the size ranges considered are the same. Originally, the classic Dergaugin, Landau, Verwey, and Overbeek (DLVO) model was evoked to explain the ability of ILs to effectively stabilize metal NPs. This model was, however, ruled out by Finke and Ott [89]. Dupont *et al.* established the importance of charged ionic aggregates localized at the surface of Ir and Rh NPs to explain their stability [90]. As a consequence, molecular features of ILs have a direct impact on the properties of metal NPs [46]. Janiak and coworkers established that Ag, Cr, Mo, and W NPs in imidazolium-based ILs have a size directly dependent upon the size of the IL counter anions, taken in the following series $^{-}BF_4$, $^{-}PF_6$, $^{-}N(O_2SCF_3)_2$, and $^{-}O_3SCF_3$ [91, 92]. With Ru NPs, Santini and coworkers explored the relationship between the size of the NPs and the alkyl chain length of imidazolium ILs used as synthetic medium [70]. For alkyl chains C_n, with $n = 4$, 6, or 8, a clear trend was observed with increased NP size being correlated with longer chains. Here the alkyl chain length correlates positively with the size of hydrophobic nanodomains in the IL, where the Ru precursor can accumulate before reduction. The relationship did not work for very short (C_2) or very long (C_{10}) chains, where other phenomena were predominant. Our group studied the impact of the properties of ILs on the resulting NPs size, catalytic performance, and longevity, using a series of phosphonium and imidazolium-based ILs [71]. Ru NPs were produced by H_2 reduction of Ru(2-methylallyl)$_2$(COD), a salt-free precursor. In the phosphonium series, one alkyl chain on the phosphorus atom was varied in length and it was shown that the longer chains resulted in slightly smaller Ru NPs compared to the shorter ones. With one phosphonium cation, the influence of the counter anion was explored using $^{-}N(O_2SCF_3)_2$, $^{-}O_3SCF_3$, $^{-}PF_6$, and ^{-}Cl. In this case, the first two anions afforded small Ru NPs, while the other two provided much larger sizes and distributions. The resulting NPs were then tested for the hydrogenation of cyclohexene. The phosphonium ILs featuring the longer alkyl chains were associated with the most active and stable Ru NPs and could be recycled up to eight times. Walden plots of all studied ILs were acquired and revealed an interesting correlation. The least ionic ILs, which are the most likely to form ion pairs, were associated with better stability of the Ru NPs (Figure 1.3a). It was thus hypothesized that ion aggregates are responsible for the stability of the metal NPs (Figure 1.3b).

Density functional theory (DFT) calculation was used by Padua and coworkers to study the solvation of Ru NPs in ILs [24]. In this study, crystalline and noncrystalline 2 nm Ru NPs were studied *in silico* in [C_4C_1Im][Ntf$_2$] (Figure 1.4). This IL is representative of IL solvents with lipophilic C_4 chains used to stabilize Ru NPs. This study revealed that the most probable interaction between the cation and the metal surface occurs in a perpendicular fashion through the methyl group on the

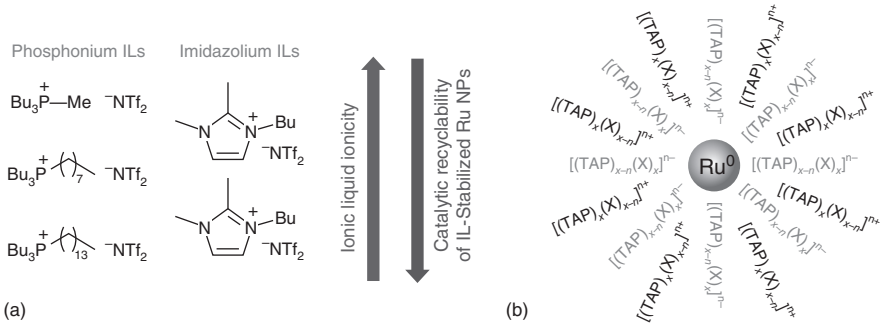

Figure 1.3 Study of Ru NPs prepared *in situ* in phosphonium and imidazolium-based ILs. (a) Correlation between IL ionicity and Ru recyclability under catalytic conditions. (b) Schematic representation of the stabilization mechanism of Ru NPs by phosphonium IL supramolecular aggregates. (TAP, tetraalkylphosphonium; $^{-}$X, counter anion.) (Luska and Moores [71]. Reproduced with the permission of Royal Society of Chemistry.)

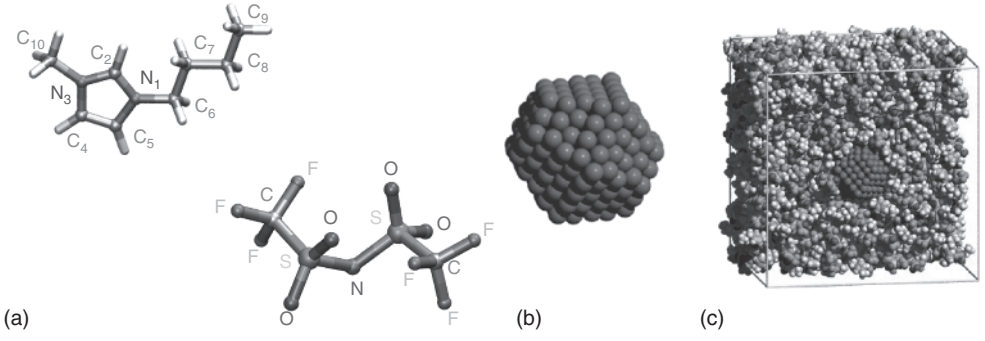

Figure 1.4 Hcp crystalline 2 nm Ru NPs (hcp crystalline) within $[C_4C_1im][Ntf_2]$ simulated using DFT methods (a) $[C_4C_1Im][Ntf_2]$ IL structure, (b) Ru NPs, and (c) Ru NPs solvated in 828 ion pairs of $[C_4C_1Im][Ntf_2]$. (Pensado and Padua [24]. Reproduced with the permission of John Wiley and Sons.)

N_3 atom. Interestingly, both the cation and anion interact directly with the surface, confirming the ionic aggregate model detailed above and further revoking the DLVO model.

1.4 Applications of Ru, Fe, and Os Nanoparticles to Catalysis

NPs have been largely applied to catalysis, and have been described as being a bridge between homogeneous and heterogeneous catalytic systems [37]. They combine the activity, selectivity, and efficacy under moderate reaction conditions

of the homogeneous systems to the easy separation, recyclability, and affordability of the heterogeneous ones. ILs are one of many supports used for metal NPs, where they not only act as stabilizers for the metal NPs but also act as the reaction medium or solvent. ILs have been studied as more sustainable solvents as they have a negligible vapor pressure and low flammability. In such systems, the ILs constitute a noninnocent catalytic medium for a number of reasons: (i) the intrinsic ability of ILs to stabilize NPs helps maintaining their small and usually more active size compared to conventional media; (ii) the intrinsic properties of the ILs, as well as the way they interact with the catalytically active NP surface, have been shown to enable unusually high activity and selectivity (*vide supra*); and (iii) the tunability of the ILs is also a major advantage in the field of catalysis, exploited notably to tweak the selectivity of catalytic systems for biomass conversion (see, for instance, Section 1.4.1.4). As a result, NPs of many transition metals have been synthesized in ILs and consequently used for catalytic applications. In this chapter, we focus on applications of Ru, Fe, and Os NPs to catalysis. In the last decade, Ru NPs in ILs have been the focus of an intense research effort [56]. Fe has been less studied, but recent results on selective hydrogenation will probably lead to more developments [73]. Although a few instances of synthesis of Os NPs in ILs were reported, no application to catalysis has been developed to the best of our knowledge.

1.4.1 Applications of Ru NPs in ILs to Catalysis

Ru-catalyzed reactions have significantly contributed to various organic transformations, such as reduction, oxidation, isomerization, and carbon–carbon bond formation [56, 93]. ILs have been combined to Ru NPs and the resulting systems have featured unique catalytic behavior with remarkable chemoselectivities, milder reaction conditions, easy recovery, and recyclability of the expensive catalyst from the reaction without any significant loss of activity. Table 1.1 summarizes the reactions carried out using NPs of Ru and Ru alloys in ILs. Ru NPs in ILs have mainly been used for hydrogenation of olefins, arenes, ketones, nitriles, and nitrobenzene, transfer hydrogenation, hydrogenolysis, dehydration, Fischer-Tropsch synthesis, methanol oxidation, isotope exchange, and biomass conversion. In the subsequent sections, we shall review these reactions in detail.

1.4.1.1 Hydrogenation of Olefins

Ru NPs in ILs have been extensively used in the catalysis of hydrogenation reactions. In 2004, they were first used by Rossi *et al.* for hydrogenation of 1-hexene. Ru NPs (2.0–2.5 nm) in 1-*n*-butyl-3-methylimidazolium ILs catalyzed the hydrogenation of 1-hexene at 75 °C, 4 bar H_2 pressure in 10 h with 99% conversion rates [110]. Although the RuO_2 hydrous precursor when used under solventless conditions gave higher reactivity than in the IL, the reaction in ILs could be recycled several times without any loss of activity. Rossi *et al.* also synthesized RuO_2 NPs, 2–3 nm in size, using $RuCl_3$ as precursor dissolved in

Table 1.1 List of reactions catalyzed by Ru and Ru alloy NPs in ILs.

Entry	Metal (size in nm)	Ionic liquid	Support	Catalyzed reaction	References
1	Ru NPs (1.7)	$[C_4C_1Im][PF_6]$ $[C_4C_1Im]_3[tppt]$	—	Nitrobenzene hydrogenation	Wu and Jiang [94]
2	Ru NPs (2.2)	$[C_4C_1Im][tppm]$	—	Aromatic ketones and aldehydes and quinolines C=O chemoselective hydrogenation	Jiang and Zheng [81]
3	Ru NPs (1.7 ± 0.4)	$[(C_4SO_3H)C_4Im]$-$[NTf_2]$	SiO_2	Biomass substrates selective deoxygenation	Luska *et al.* [95]
4	Ru NPs ($6.9 \pm 1.$)	$[C_1C_1(EG)Im][NTf_2]$	—	Partial hydrogenation of C=O and C=C bonds	Darwich *et al.* [83]
5	Ru NPs (1.4–5.0)	$[P_{4,4,4,1}]NTf_2$ $[P_{4,4,4,8}]NTf_2$ $[P_{4,4,4,14}]X$ $(X = NTf_2, OTf, PF_6)$ $[C_4C_1Im][NTf_2]$ $[C_2C_1C_1Im][NTf_2]$	—	Cyclohexene hydrogenation	Luska and Moores [71]
6	Ru NPs (1.4–4.1)	$[C_4C_1Im]X$ $[C_4Py]X$ $(X = OAc, DCA, BF_4, OTf, MeHPO_3)$	Al_2O_3	Benzene to cyclohexene selective hydrogenation	Schwab *et al.* [96]
7	Ru NPs (3.5 ± 0.6)	$[C_{12}C_1Im][NTf_2]$	—	Furfuryl alcohol to tetrahydrofurfuryl alcohol hydrogenation	Geilen *et al.* [97]
8	Ru NPs (1.2)	$[C_4C_1Im][NTf_2]$	$C_nH_{2n+1}NH_2$ $(n = 6,8)$	Toluene hydrogenation (low conversions)	Salas *et al.* [98]
9	Ru NPs (2.2 ± 0.4)	$[C_4C_1Im][BF_{4]}$	Graphene	Cyclohexene and benzene hydrogenation	Marquardt *et al.* [77]
10	Ru NPs (4.0)	$[C_4C_1Im][PF_6]$ $[P_{6,6,6,14}][DBS]$	—	Cellulose to hexitols hydrogenation	Zhu *et al.* [99]

(*continued overleaf*)

Table 1.1 (*Continued*).

Entry	Metal (size in nm)	Ionic liquid	Support	Catalyzed reaction	References
11	Ru NPs (2–3)	Brønsted acid-functionalized $[C_4C_1Im][BF_4]$	—	Dehydration/ hydrogenation of phenol into hexane	Yan *et al.* [100]
12	Ru NPs (<5)	$[C_4C_1Im][BF_4]$	—	Cyclohexene hydrogenation	Vollmer *et al.* [76]
13	Ru NPs (2.7)	$[C_2C_1Im][X]$ $X = NTf_2$, *OAc*, *Br* $[C_4C_1Im][BF_4]$ $[C_{12}C_1Im][NTf_2]$ $[C_2C_1C_1Im][NTf_2]$	—	Biomass-derived 4-(2-furyl)-3-butene-2-one selective hydrogenation	Julis *et al.* [101]
14	Ru NPs (1.1–2.9)	$[C_4C_1Im][NTf_2]$	—	1,3-Cyclohexadiene selective hydrogenation	Campbell *et al.* [68]
15	Ru NPs (2.0 ± 0.3)	$[C_4Im][NTf_2]$ $[C_6C_1Im][NTf_2]$	—	Toluene hydrogenation	Prechtl *et al.* [72]
16	Ru NPs (2.7 ± 0.4)	$[C_4C_1Im][PF_6]$ $[C_4C_1Im][BF_4]$ $[C_4C_1Im][OTf]$	—	Arene hydrogenation	Rossi and Machado [102]
17	Ru–Cu (5–8)	[TMG][Lactate]	Bentonite clay	Glycerol to 1,2-propanediol hydrogenolysis	Jiang *et al.* [103]
18	Ru NPs (2.2 ± 0.5)	$[(C_3CN)C_1Im][NTf_2]$	—	Aromatic nitriles selective hydrogenation	Prechtl *et al.* [82]
19	Ru NPs (2.0 ± 0.2)	$[C_4C_1Im][BF_4]$	PVP	Fischer–Tropsch synthesis	Xiao *et al.* [13]
20	Ru NPs (2.1–3.5)	$[C_4C_1Im][NTf_2]$	—	Arene hydrogenation	Prechtl *et al.* [65]
21	Ru NPs (<2)	Choline hydroxide	MgO	Acetophenone transfer hydrogenation	Kantam *et al.* [104]
22	Ru NPs (2.6)	$[C_4C_1Im][PF_6]$	—	Isotope exchange	Yinghuai *et al.* [105]
23	Ru NPs (2.4 ± 0.4)	$[C_4C_1Im][Cl]$	PVP	Cellobiose to C6-alcohols conversion	Yan *et al.* [106]

Table 1.1 (*Continued*).

Entry	Metal (size in nm)	Ionic liquid	Support	Catalyzed reaction	References
24	Ru NPs (<3)	[TMG][TFA]	Montmorillonite clay	Benzene hydrogenation	Miao *et al.* [107]
25	Pt-Ru (2.5–3.5)	$[C_4C_1Im][PF_6]$	Carbon black	Methanol oxidation	Xue *et al.* [108]
26	Ru NPs (2–5)	[TMG][Lactate]	SBA-15	Arene hydrogenation	Huang *et al.* [109]
27	Ru NPs (2.6 ± 0.4)	$[C_4C_1Im][PF_6]$ $[C_4C_1Im][BF_4]$ $[C_4C_1Im][OTf]$	—	Benzene to cyclohexene, olefin hydrogenations	Silveira *et al.* [67]
28	Ru NPs (2.0–2.5)	$[C_4C_1Im][X]$ $X = PF_6$, BF_4, OTf	—	1-Hexene hydrogenation	Rossi *et al.* [110]
29	RuO_2 NPs (2–3)	$[C_4C_1Im][PF_6]$ $[C_4C_1Im][BF_4]$	—	Olefins and arenes hydrogenation	Rossi *et al.* [66]

C_1, C_2, C_4, methyl, ethyl, butyl, and so on; C_3CN, butyronitrile; C_4SO_3H, butylsulfonic acid; $C_nC_{n'}Im$, 1,3 functionalized imidazolium; $C_nC_{n'}C_{n''}Im$, 1,2,3 functionalized imidazolium; $[C_4C_1Pyr]$, 1-butyl-1-methylpyrrolidinium; OTf, trifluoromethanesulfonate; NTf_2, bis(trifluoromethylsulfonyl)imide; TMG, 1,1,3,3-tetramethylguanidinium; DCA, dicyanamide; PVP, poly(*N*-vinyl-2-pyrrolidone); TFA, trifluoroacetate; OAc, acetate; tppt, tri(*m*-sulfonyl)triphenyl phosphine; tppm, *m*-sulfonyltriphenyl phosphine; DBS, dodecylbenzene sulfonate; $C_1C_1(EG)Im$ = 1-(2,3-dihydroxypropyl)-2,3-dimethylimidazolium.

1-*n*-butyl-3-methylimidazolium ILs [66]. These NPs were then utilized for the hydrogenation of 1-hexene at 75 °C, 4 bar H_2, with a total turnover number for exposed Ru atoms of 175 000 and recyclable up to 10 times. Thereafter, several results were published demonstrating the role of Ru NPs in ILs for olefin hydrogenation, for example, those obtained by Silveira *et al.* [67], Vollmer *et al.* [76], Marquardt *et al.* [77], and Luska and Moores [71]. Luska and Moores, for instance, showed the dependence of catalyst stability and activity on the ionicity of the IL (Scheme 1.2a, Figure 1.4) [71]. Ru NPs (1.4–5.0 nm) were synthesized in a series of phosphonium and imidazolium ILs for direct comparison of the catalytic activity of Ru NPs in ILs of different ionicities in the hydrogenation of cyclohexene at 75 °C and 4 bar H_2. The ionicities of the phosphonium and imidazolium ILs were determined from a Walden plot analysis, which indicated that the most stable Ru NPs were synthesized in ILs having the lowest ionicity. Stabilization of the NPs was provided by the strong associations between the IL anion and cation and the resulting formation of ionic aggregates. Phosphonium ILs demonstrated higher activities and recyclabilities than imidazolium ILs. They showed that in the phosphonium ILs, the recyclability was dependent on the length of the P-alkyl chain. By increasing the length of the chain, the durability of the catalyst could be

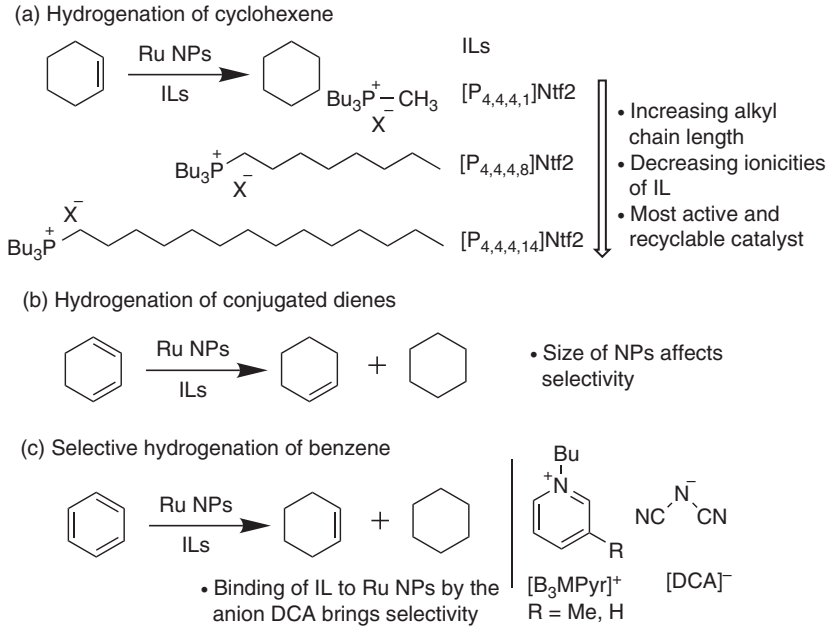

Scheme 1.2 Selected hydrogenation reactions catalyzed by Ru NPs in ILs: (a) hydrogenation of cyclohexene, (b) hydrogenation of conjugated diene, 1,3-cyclohexadiene, and (c) selective hydrogenation of benzene.

increased. Hydrogenation of a conjugated diene, 1,3-cyclohexadiene, by Ru NPs in imidazolium ILs was studied by Campbell *et al.* to compare the factors that lead to the partially hydrogenated product, cyclohexene, and the fully hydrogenated product, cyclohexane (Scheme 1.2b) [68]. They studied the catalysis with different sizes of Ru NPs (1.1, 2.3, 2.9 nm) in ILs and deduced that the larger Ru NPs possessed higher activity for the hydrogenation of 1,3-cyclohexadiene, but the smaller Ru NPs gave higher selectivity of the partially hydrogenated product, cyclohexene.

1.4.1.2 Hydrogenation of Arenes

Another wide application of Ru NPs in ILs is the hydrogenation of arenes [49, 65, 72, 102, 107]. A highly efficient heterogeneous catalyst was prepared for hydrogenation of benzene to cyclohexane by Miao *et al.* in 2006 by synthesizing Ru NPs immobilized on montmorillonite (MMT) clay by the IL 1,1,3,3-tetramethylguanidinium trifluoroacetate [107]. In their system, they obtained two kinds of Ru NPs, one on the MMT surface, of size about 3 nm, and another in the interlayers of MMT, of size less than 1.2 nm. Both types of NPs were active in catalysis. However, aggregation of surface NPs after five catalysis cycles, while the activity of the system was maintained, proved that the interior Ru NPs played the main role in this reaction. Prechtl *et al.* also carried out the hydrogenation of arenes with Ru NPs (2.1–3.5 nm) in imidazolium ILs, with the ability to be reused several times [65]. Their system was sensitive to the steric effect imposed by alkyl groups on the aromatic rings, with

higher substituted arenes (e.g., xylenes) resulting in lower yields as compared to benzene and toluene. They studied the kinetics of the reaction by generating Arrhenius plots for the hydrogenation of toluene and deduced an activation energy, E_A, of 42.0 kJ mol^{-1} in the biphasic liquid–liquid system with Ru NPs in $[C_4C_1Im][NTf_2]$. Notably, this is analogous to the activation energies reported for the transition-metal-catalyzed hydrogenation of toluene (40–50 kJ mol^{-1}) with solid-phase metal catalysts on solid supports. In another work, Prechtl *et al.* also synthesized Ru NPs in NTf_2 imidazolium ILs from the organometallic complex, [Ru(COD)(2-methylallyl)$_2$], without using any external reducing agent (see Section 1.2.1) [72]. The resulting Ru NPs produced in $[C_6C_1C_1Im][NTf_2]$ showed the highest activity for hydrogenation of toluene at 4 bar H_2 at 75 °C in 18 h with conversions over 95%.

Under hydrogenation conditions, benzene usually converts into the completely hydrogenated product, cyclohexane, which is the most thermodynamically stable. The product of the partial hydrogenation, cyclohexene, is an important industrial intermediate, justifying intense research to obtain it from benzene. Interestingly, Ru NPs in ILs have shown superior ability in this challenging reaction, although the cyclohexene yield and selectivity reported so far are too low for commercial development. In 2004, Silveira *et al.* achieved up to 39% selectivity for cyclohexene at very low benzene conversion by Ru NPs in imidazolium ILs [67]. Similarly, Rossi *et al.* achieved a maximum selectivity to cyclohexene of 65%, at 0.3% of benzene conversion, at 120 °C and 4 atm H_2 in the $[C_4C_1Im][BF_4]$ IL biphasic system [102]. Schwab *et al.* demonstrated that addition of IL, $[C_4Py][DCA]$ (DCA = dicyanamide), to the Ru NPs supported on Al_2O_3 could result in selective hydrogenation of benzene (Scheme 1.2c, DCA = $N(CN)_2$) [96]. They carried out a systematic study of the effect of amount of IL added to the reaction and the Ru NP size on the selectivity of the reaction. They deduced that the IL binds to the Ru NP surface through the $^-N(CN)_2$ anions and these ensembles slow down the reaction to enable the desired selectivity.

1.4.1.3 Other Types of Hydrogenations

Ru NPs (<2 nm) stabilized on nanocrystalline magnesium oxide with ILs were used for transfer hydrogenation of carbonyl compounds at 85 °C in isopropanol in the presence of 0.1 M KOH by Kantam *et al*. [104] Recently, Jiang e*t al.* established the use of Ru NPs (2.2 nm) stabilized by phosphine-functionalized ILs in the chemoselective hydrogenation of aromatic ketones, aromatic aldehydes, and quinolines with switchable selectivity toward different functional groups of the substrates (Scheme 1.3a) [81]. Their results demonstrated the role of the phosphine-stabilized ILs in modification of Ru NPs in chemoselective hydrogenation in addition to the stabilization of the Ru NPs in the preparation of the catalyst. Moreover, the use of water as solvent resulted in a different set of hydrogenated products compared to the solventless reaction.

Prechtl *et al.* showed that the selective hydrogenation of aromatic nitriles could be achieved by Ru NPs (2.2 nm ± 0.5 nm) in nitrile-functionalized 1-butyronitrile-3-methylimidazolium bis(trifluoromethane-sulfonyl)-imidate ILs (Scheme 1.3b) [82]. The hydrogenation product, benzylamine, was rapidly transformed via

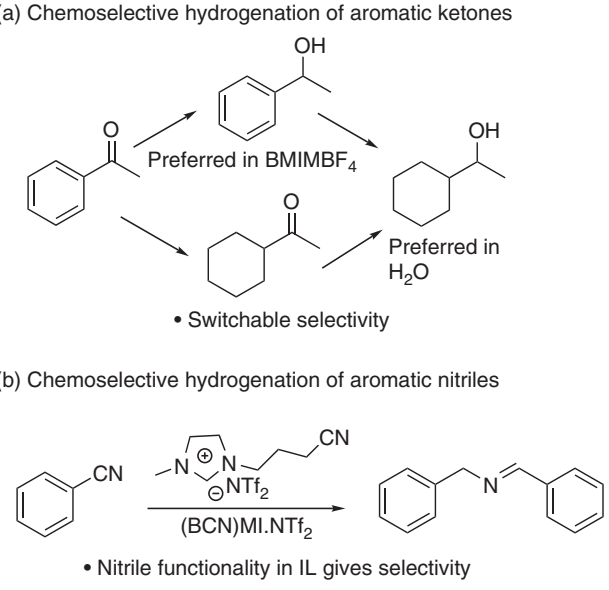

Scheme 1.3 Chemoselective hydrogenation of (a) aromatic ketones and (b) aromatic nitriles catalyzed by Ru NPs in ILs.

aminolysis and coupling into benzylidene benzylamine. Interestingly, no hydrogenation of the aromatic ring was observed and it was hypothesized that the nitrile group of the IL coordinated as a ligand to the metal surface, forming an IL layer and blocking the surface for interactions with arenes. Selective hydrogenation of nitrobenzene and other aromatic nitro compounds to aniline and other corresponding aromatic amines, respectively, has also been carried out by Ru NPs (1.7 nm) stabilized by phosphine-functionalized ILs at 60 °C and 5 MPa H_2 [94]. Another example of selective hydrogenation was provided by Prechtl, Santini, and coworkers who produced Ru NPs in a dihydroxyl-functionalized imidazolium IL $[C_1C_1(EG)Im][NTf_2]$ as solvent and stabilizer. This system proved a selective partial hydrogenation catalyst to transform α,β-unsaturated compounds such as cyclohexenone and cinnamic aldehyde into their corresponding unsaturated alcohols or saturated alcohols [83].

1.4.1.4 Biomass Conversion

The affordable and sustainable conversion of biomass into fuels and commodity chemicals is currently a major technological challenge. Ru NPs stabilized in ILs have unlocked novel catalytic transformations and processes for biomass conversion [26]. Yan *et al.* achieved the one-step conversion of cellobiose to C6-alcohols by selectively breaking the C–O–C bonds via selective hydrogenation using a water-soluble Ru nanocluster catalyst (2.4 ± 0.4 nm) in $[C_4C_1Im][Cl]$ under 40 bar H_2 pressure at 120 °C in 12 h [106]. Although low conversions of 15% were observed, this reaction is proof of concept for novel processes in

biomass conversion. Jiang *et al.* carried out the hydrogenolysis of glycerol to 1,2-propanediol (1,2-PDO), catalyzed by a bimetallic Ru-Cu catalyst (5–8 nm), supported on bentonite clay with the help of an IL [103]. Specifically, the clay was modified with a functional IL, 1,1,3,3-tetramethylguanidinium lactate ([TMG][Lactate]), before the bimetallic NPs were deposited onto it. The catalyst was used for hydrogenolysis of an aqueous solution of glycerol at 190–240 °C and 2.5–10 MPa H_2. The catalytic system was both efficient and selective, achieving 100% of glycerol conversion and 85% yield of 1,2-PDO at 230 °C and 8 MPa H_2. The molar ratio of Ru/Cu played a vital role in the selectivity of the reaction. On decreasing the molar ratio of Ru to Cu, the conversion of glycerol gradually decreased while the selectivity towards liquid products and the content of 1,2-PDO in the collected liquid increased. The conversion of glycerol and the selectivity to 1,2-PDO did not decrease after the catalyst was used five times. Julis *et al.* carried out selective hydrogenation of the biomass-derived 4-(2-furyl)-3-butene-2-one by Ru NPs (2.7 nm), synthesized and stabilized in a variety of imidazolium-based ILs [101]. ILs with variable alkyl chain length and varied substituents at the C2-position were used. A set of anions differing in their nucleophilicity and coordination strength were also checked. At 120 bar and 120 °C, all catalytic systems gave more than 99% conversions, although the product distribution differed depending on the IL. The selectivity was only moderately influenced by the alkyl chain length in the imidazolium cation as compared by the anion of IL. Dehydration of phenols into cyclohexanes was studied by Yan *et al.* as a model for the conversion of lignin-derived molecules into alkanes under mild conditions [100]. In this process, several hydrogenation steps are required, which could be catalyzed by Ru NPs, while a dehydration step calls for the use of a Brønsted acid. Ru NPs (2–3 nm) were thus prepared directly within ILs featuring a Brønsted acid covalently linked to the IL cation via an alkyl chain. The dehydration step was studied individually and it was found that the acidity of the IL was positively correlated with catalytic activity, the best systems being the SO_3H-functionalized IL. Ru NPs in the SO_3H-functionalized IL allowed to convert, with exceptionally high selectivity (97%), phenol to cyclohexane at 40 atm H_2, 130 °C, and in 4 h. Rh NPs in the same IL achieved better activity, but at the expense of selectivity. A similar approach with acid-functionalized ILs was used by Luska *et al.* for selective deoxygenation of biomass substrates [95]. Ru NPs (1.7 ± 0.4 nm) were immobilized onto silica in a scheme referred to as supported ionic liquid phase (SILP), where the IL used was acid functionalized and afforded a bifunctional catalyst. The system showed high catalytic activities, selectivities, and recyclabilities in the hydrogenolytic deoxygenation of 4-(2-tetrahydrofuryl)-2-butanol and of 4-(5-(hydroxymethyl)-2-tetrahydrofuryl)-2-butanol, where the product selectivity toward 2-butyltetrahydrofuran, 1-octanol, or 1,1-dioctylether could be achieved by controlling the reaction conditions and acidity of the SILPs. Zhu *et al.* used Ru NPs (4.0 nm) stabilized in ILs in the presence of a reversible boronic binding group for conversion of cellulose to hexitols at 80 °C, 10 bar H_2 in 5 h with yields up to 95% [99]. The system relied on a reversible boronic acid binding agent that aided in breaking the crystal packing of cellulose by

reversible binding with the multiple hydroxyl groups to improve solubility and catalytic activity. Geilen *et al.* studied the hydrogenation of furfuryl alcohol to tetrahydrofurfuryl alcohol with Ru NPs (3.5 ± 0.6 nm) in imidazolium ILs at 100 bar H_2 and 150 °C in 16 h with 100% conversion and 95% selectivity [97].

1.4.1.5 Miscellaneous Reactions

In addition to the hydrogenation reaction, a characteristic application of Ru NPs in ILs, several examples of other reactions were reported in the literature, for example, methanol oxidation [108], isotope exchange [105], and Fischer-Tropsch synthesis [13]. Xue *et al*. used a bimetallic Pt-Ru (2.5–3.5 nm) catalyst immobilized on carbon in IL as the anodic fuel cell in a direct methanol fuel cell (DMFC) [108]. The work showed that the average crystal size, relative crystallinity, and chemical states of the metal particles in the catalyst affected the electrocatalytic activity of the catalyst. The catalytic systems with low relative crystallinity and higher surface areas proved to be highly active for methanol oxidation. In another work, Ru NPs (2.6 nm) in phosphonium ILs were shown to catalyze the isotope exchange reaction between ^{10}B-enriched diborane and natural abundant $B_{10}H_{14}$ to produce highly ^{10}B-enriched (~90%) decaborane [105]. Xiao *et al.* used Ru NPs (2.0 ± 0.2 nm) synthesized in the presence of poly(*N*-vinyl-2-pyrrolidone) (PVP) and imidazolium ILs in Fischer-Tropsch synthesis and demonstrated that the Ru NPs in IL had better catalytic activities when compared to the conventional Ru NP catalysts, where the support effects greatly alter the catalysis [13].

1.4.2 Applications of Fe Nanoparticles to Catalysis

Examples of applications of IL-supported Fe NPs in catalysis are scarce. Gieshoff *et al.* demonstrated the use of FeNPs (4–5 nm) in imidazolium ILs in selective hydrogenation of alkynes to the partially hydrogenated product, alkene, at 60 bar H_2, 80 °C in 2 days (Scheme 1.4) [73]. They could achieve a selective cis-hydrogenation when the IL had a nitrile function, suppressed N-heterocyclic carbene formation, and the solvent used was heptane, instead of THF. The catalyst was robust for recycling, and gave high activity and selectivity for up to eight cycles.

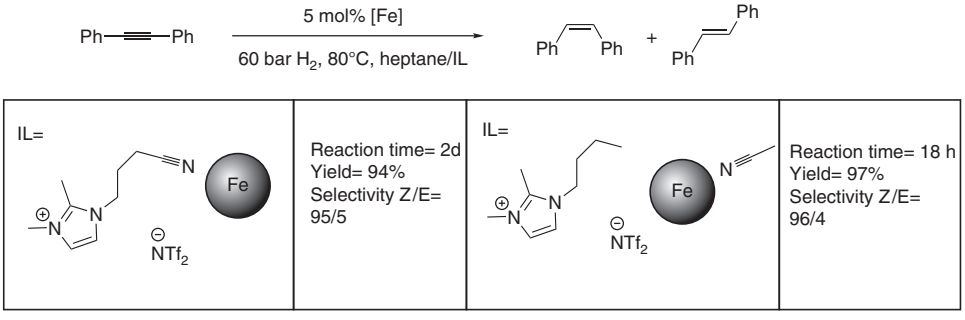

Scheme 1.4 Selective hydrogenation of alkynes with Fe NPs in ILs.

1.5 Conclusion

To summarize, the synthesis of NPs for Fe, iron oxide, Ru, and Os could be accomplished under mild conditions in ILs by either reduction or decomposition. Unlike traditional aqueous and organic media, ILs provide structural support for the formation and stabilization of small NPs. The mechanism(s) at play for this effect is not fully understood, but various studies described above point toward the nanoscale structure of ILs, the important role of the formation of ion aggregates, and charged interactions between the IL components and the NP surface. In catalysis, these systems have proved to be particularly efficient for effective reactions under mild conditions and high selectivity. Ru NPs have been intensely researched, revealing a few important traits. First, ILs allow to maintain the small size and thus the activity of the metal NPs throughout multiple recyclings. Second, ILs may be tuned or equipped with other functionalities to unlock novel reactivities. Lastly, they allow easy recovery via simply biphasic separation. These features have made IL-stabilized NPs ideal catalysts for the challenging biomass conversion reactions or for discoveries in the field of fuel cells, although further improvements are necessary before industrial requirements can be met. In this area, Ru has been the main focus of attention, but Fe, as a nontoxic, readily available, and cheap metal, is now attracting increasing interest.

Acknowledgments

We thank the Natural Science and Engineering Research Council of Canada (NSERC) Discovery Grant program, the Canada Foundation for Innovation (CFI), the Canada Research Chairs (CRC), the Centre for Green Chemistry and Catalysis (CGCC), NSERC-Collaborative Research and Training Experience (CREATE) in Green Chemistry, and McGill University for their financial support.

References

1. Fürstner, A. (2009) *Angew. Chem. Int. Ed.*, **48**, 1364–1367.
2. Junge, K., Schröder, K., and Beller, M. (2011) *Chem. Commun.*, **47**, 4849–4859.
3. Czaplik, W.M., Mayer, M., Cvengroš, J., and Jacobi von Wangelin, A. (2009) *ChemSusChem*, **2**, 396–417.
4. Welther, A. and Jacobi von Wangelin, A. (2013) *Curr. Org. Chem.*, **17**, 326–335.
5. Hudson, R., Feng, Y., Varma, R.S., and Moores, A. (2014) *Green Chem.*, **16**, 4493–4505.
6. Plietker, B. (2008) *Iron Catalysis in Organic Chemistry: Reactions and Applications*, Wiley-VCH Verlag GmbH, Weinheim.
7. Bart, S.C., Lobkovsky, E., and Chirik, P.J. (2004) *J. Am. Chem. Soc.*, **126**, 13794–13807.
8. Punniyamurthy, T., Velusamy, S., and Iqbal, J. (2005) *Chem. Rev.*, **105**, 2329–2364.
9. Enthaler, S., Junge, K., and Beller, M. (2008) *Angew. Chem. Int. Ed.*, **47**, 3317–3321.

10. Schlögl, R. (2003) *Angew. Chem. Int. Ed.*, **42**, 2004–2008.
11. Fryzuk, M.D. (2004) *Nature*, **427**, 498–499.
12. Schulz, H. (1999) *Appl. Catal., A*, **186**, 3–12.
13. Xiao, C.x., Cai, Z.P., Wang, T., Kou, Y., and Yan, N. (2008) *Angew. Chem. Int. Ed.*, **120**, 758–761.
14. Morris, R.H. (2007) *The Handbook of Homogeneous Hydrogenation* (ed. J.G. de Vries), Wiley-VCH Verlag GmbH & Co. KGaA, Weinheim, pp. 45–70.
15. Grubbs, R.H. and O'Leary, D.J. (2015) *Handbook of Metathesis: Applications in Organic Synthesis*, Wiley-VCH Verlag GmbH, Weinheim.
16. Arockiam, P.B., Bruneau, C., and Dixneuf, P.H. (2012) *Chem. Rev.*, **112**, 5879–5918.
17. Pappo, R., Allen, D. Jr.,, Lemieux, R., and Johnson, W. (1956) *J. Org. Chem.*, **21**, 478–479.
18. Sánchez-Delgado, R.A., Rosales, M., Esteruelas, M.A., and Oro, L.A. (1995) *J. Mol. Catal. A: Chem.*, **96**, 231–243.
19. Chelucci, G., Baldino, S., and Baratta, W. (2015) *Acc. Chem. Res.*, **48**, 363–379.
20. Low, J.E., Foelske-Schmitz, A., Krumeich, F., Wörle, M., Baudouin, D., Rascón, F., and Copéret, C. (2013) *Dalton Trans.*, **42**, 12620–12625.
21. Lam, V.W. and Gyenge, E.L. (2008) *J. Electrochem. Soc.*, **155**, B1155–B1160.
22. Weingärtner, H. (2008) *Angew. Chem. Int. Ed.*, **47**, 654–670.
23. Dupont, J. (2011) *Acc. Chem. Res.*, **44**, 1223–1231.
24. Pensado, A.S. and Padua, A.A. (2011) *Angew. Chem. Int. Ed.*, **50**, 8683–8687.
25. Olivier-Bourbigou, H., Magna, L., and Morvan, D. (2010) *Appl. Catal., A*, **373**, 1–56.
26. Luska, K., Migowski, P., and Leitner, W. (2015) *Green Chem.*, **17**, 3195–3206.
27. Schubert, T.J. (2013) *Supported Ionic Liquids: Fundamentals and Applications* (eds R. Fehrmann, A. Riisager, and M. Haumann), Wiley-VCH Verlag GmbH & Co. KGaA, Weinheim, pp. 445–456.
28. McCrary, P.D., Beasley, P.A., Cojocaru, O.A., Schneider, S., Hawkins, T.W., Perez, J.P.L., McMahon, B.W., Pfeil, M., Boatz, J.A., and Anderson, S.L. (2012) *Chem. Commun.*, **48**, 4311–4313.
29. Schneider, S., Hawkins, T., Rosander, M., Vaghjiani, G., Chambreau, S., and Drake, G. (2008) *Energy Fuels*, **22**, 2871–2872.
30. Welton, T. (2004) *Coord. Chem. Rev.*, **248**, 2459–2477.
31. Crowhurst, L., Mawdsley, P.R., Perez-Arlandis, J.M., Salter, P.A., and Welton, T. (2003) *Phys. Chem. Chem. Phys.*, **5**, 2790–2794.
32. Dupont, J., Fonseca, G.S., Umpierre, A.P., Fichtner, P.F., and Teixeira, S.R. (2002) *J. Am. Chem. Soc.*, **124**, 4228–4229.
33. Cole-Hamilton, D.J. (2003) *Science*, **299**, 1702–1706.
34. Bell, A.T. (2003) *Science*, **299**, 1688–1691.
35. Geukens, I. and De Vos, D.E. (2013) *Langmuir*, **29**, 3170–3178.
36. Dupont, J. and Scholten, J.D. (2010) *Chem. Soc. Rev.*, **39**, 1780–1804.
37. Astruc, D. (2008) *Nanoparticles and Catalysis*, Wiley-VCH Verlag GmbH & Co KGaA, Weinheim.
38. Astruc, D., Lu, F., and Aranzaes, J.R. (2005) *Angew. Chem. Int. Ed.*, **44**, 7852–7872.
39. Pârvulescu, V.I. and Hardacre, C. (2007) *Chem. Rev.*, **107**, 2615–2665.
40. Dyson, P.J., Fei, Z.F., Geldbach, T.J., and Zhao, D.B. (2006) *Chem. Eur. J.*, **12**, 2123–2130.
41. Lee, S.G. (2006) *Chem. Commun.*, **14**, 1049–1063.
42. Luska, K.L. and Moores, A. (2012) *ChemCatChem*, **4**, 1534–1546.
43. Neouze, M.-A. (2010) *J. Mater. Chem.*, **20**, 9593–9607.
44. Vollmer, C. and Janiak, C. (2011) *Coord. Chem. Rev.*, **255**, 2039–2057.
45. Dupont, J. and Meneghetti, M.R. (2013) *Curr. Opin. Colloid Interface Sci.*, **18**, 54–60.
46. Lignier, P. (2015) *Topics in Organometallic Chemistry*, Springer, Berlin, Heidelberg.
47. Dyson, P.J. and Geldbach, T.J. (2005) *Metal Catalysed Reactions in Ionic Liquids*, vol. **29**, Springer, Dordrecht.

48. Migowski, P. and Dupont, J. (2007) *Chem. Eur. J.*, **13**, 32–39.
49. Dupont, J. and de Oliveira Silva, D. (2008) *Nanoparticles and Catalysis* (ed. D. Astruc), Wiley-VCH Verlag GmbH & Co. KGaA, Weinheim, pp. 195–218.
50. Kou, Y., Yan, N., and Xiao, C.X. (2010) *Coord. Chem. Rev.*, **254**, 1179–1218.
51. Scholten, J.D., Leal, B.C., and Dupont, J. (2011) *ACS Catal.*, **2**, 184–200.
52. Prechtl, M.H.G. and Campbell, P.S. (2013) *Nanotechnol. Rev.*, **2**, 577–595.
53. Scholten, J.D. and Dupont, J. (2014) *Hydrogenation with Nanoparticles Using Supported Ionic Liquids*, Wiley-VCH Verlag GmbH & Co KGaA, Weinheim.
54. Zhang, P., Wu, T., and Han, B. (2014) *Adv. Mater.*, **26**, 6810–6827.
55. Zhang, B. and Yan, N. (2013) *Catalysts*, **3**, 543–562.
56. Campbell, P.S., Prechtl, M.H.G., Santini, C.C., and Haumesser, P.-H. (2013) *Curr. Org. Chem.*, **17**, 414–429.
57. Zhao, D., Fei, Z., Ang, W.H., and Dyson, P.J. (2006) *Small*, **2**, 879–883.
58. Itoh, H., Naka, K., and Chujo, Y. (2004) *J. Am. Chem. Soc.*, **126**, 3026–3027.
59. Mévellec, V., Leger, B., Mauduit, M., and Roucoux, A. (2005) *Chem. Commun.*, **41**, 2838–2839.
60. Antonietti, M., Kuang, D., Smarsly, B., and Zhou, Y. (2004) *Angew. Chem. Int. Ed.*, **43**, 4988–4992.
61. Chaudret, B. (2005) *C.R. Phys.*, **6**, 117–131.
62. Philippot, K. and Chaudret, B. (2003) *C.R. Chim.*, **6**, 1019–1034.
63. Pan, C., Pelzer, K., Philippot, K., Chaudret, B., Dassenoy, F., Lecante, P., and Casanove, M.-J. (2001) *J. Am. Chem. Soc.*, **123**, 7584–7593.
64. Corain, B., Schmid, G., and Toshima, N. (2011) *Metal Nanoclusters in Catalysis and Materials Science: The Issue of Size Control: The Issue of Size Control*, Elsevier, Amsterdam.
65. Prechtl, M.H.G., Scariot, M., Scholten, J.D., Machado, G., Teixeira, S.R., and Dupont, J. (2008) *Inorg. Chem.*, **47**, 8995–9001.
66. Rossi, L.M., Dupont, J., Machado, G., Fichtner, P.F., Radtke, C., Baumvol, I.J., and Teixeira, S.R. (2004) *J. Braz. Chem. Soc.*, **15**, 901–910.
67. Silveira, E.T., Umpierre, A.P., Rossi, L.M., Machado, G., Morais, J., Soares, G.V., Baumvol, I.J., Teixeira, S.R., Fichtner, P.F., and Dupont, J. (2004) *Chem. Eur. J.*, **10**, 3734–3740.
68. Campbell, P.S., Santini, C.C., Bayard, F., Chauvin, Y., Collière, V., Podgoršek, A., Gomes, M.F.C., and Sá, J. (2010) *J. Catal.*, **275**, 99–107.
69. Gutel, T., Garcia-Antõn, J., Pelzer, K., Philippot, K., Santini, C.C., Chauvin, Y., Chaudret, B., and Basset, J.-M. (2007) *J. Mater. Chem.*, **17**, 3290–3292.
70. Gutel, T., Santini, C.C., Philippot, K., Padua, A., Pelzer, K., Chaudret, B., Chauvin, Y., and Basset, J.M. (2009) *J. Mater. Chem.*, **19**, 3624–3631.
71. Luska, K.L. and Moores, A. (2012) *Green Chem.*, **14**, 1736–1742.
72. Prechtl, M.H.G., Campbell, P.S., Scholten, J.D., Fraser, G.B., Machado, G., Santini, C.C., Dupont, J., and Chauvin, Y. (2010) *Nanoscale*, **2**, 2601–2606.
73. Gieshoff, T.N., Welther, A., Kessler, M.T., Prechtl, M.H.G., and von Wangelin, A.J. (2014) *Chem. Commun.*, **50**, 2261–2264.
74. Banerjee, A., Theron, R., and Scott, R.W. (2013) *Chem. Commun.*, **49**, 3227–3229.
75. Krämer, J., Redel, E., Thomann, R., and Janiak, C. (2008) *Organometallics*, **27**, 1976–1978.
76. Vollmer, C., Redel, E., Abu-Shandi, K., Thomann, R., Manyar, H., Hardacre, C., and Janiak, C. (2010) *Chem. Eur. J.*, **16**, 3849–3858.
77. Marquardt, D., Vollmer, C., Thomann, R., Steurer, P., Mülhaupt, R., Redel, E., and Janiak, C. (2011) *Carbon*, **49**, 1326–1332.
78. Lee, C.-M., Jeong, H.-J., Lim, S.T., Sohn, M.-H., and Kim, D.W. (2010) *ACS Appl. Mater. Interfaces*, **2**, 756–759.
79. Wang, Y., Maksimuk, S., Shen, R., and Yang, H. (2007) *Green Chem.*, **9**, 1051–1056.
80. Wang, Y. and Yang, H. (2009) *Chem. Eng. J.*, **147**, 71–78.

81. Jiang, H.-y. and Zheng, X.-x. (2015) *Catal. Sci. Technol.*, **5**, 3728–3734.
82. Prechtl, M.H.G., Scholten, J.D., and Dupont, J. (2009) *J. Mol. Catal. A: Chem.*, **313**, 74–78.
83. Darwich, W., Gedig, C., Srour, H., Santini, C.C., and Prechtl, M.H. (2013) *RSC Adv.*, **3**, 20324–20331.
84. Zhang, Y., Liu, D., Wang, X., Song, S., and Zhang, H. (2011) *Chem. Eur. J.*, **17**, 920–924.
85. Canongia Lopes, J.N. and Pádua, A.A. (2006) *J. Phys. Chem. B*, **110**, 3330–3335.
86. Hardacre, C., Holbrey, J.D., McMath, S.J., Bowron, D.T., and Soper, A.K. (2003) *J. Chem. Phys.*, **118**, 273–278.
87. Hardacre, C., McMath, S.J., Nieuwenhuyzen, M., Bowron, D.T., and Soper, A.K. (2003) *J. Phys.: Condens. Matter*, **15**, S159.
88. Deetlefs, M., Hardacre, C., Nieuwenhuyzen, M., Padua, A.A., Sheppard, O., and Soper, A.K. (2006) *J. Phys. Chem. B*, **110**, 12055–12061.
89. Finke, R.G. and Ott, L.S. (2007) *Coord. Chem. Rev.*, **251**, 1075–1100.
90. Dupont, J., Fonseca, G.S., Umpierre, A.P., Fichtner, P.F.P., and Teixeira, S.R. (2003) *Chem. Eur. J.*, **9**, 3263–3269.
91. Redel, E., Thomann, R., and Janiak, C. (2008) *Inorg. Chem.*, **47**, 14–16.
92. Redel, E., Thomann, R., and Janiak, C. (2008) *Chem. Commun.*, **44**, 1789–1791.
93. Naota, T., Takaya, H., and Murahashi, S.-I. (1998) *Chem. Rev.*, **98**, 2599–2660.
94. Wu, Z. and Jiang, H. (2015) *RSC Adv.*, **5**, 34622–34629.
95. Luska, K.L., Julis, J., Stavitski, E., Zakharov, D.N., Adams, A., and Leitner, W. (2014) *Chem. Sci.*, **5**, 4895–4905.
96. Schwab, F., Lucas, M., and Claus, P. (2011) *Angew. Chem. Int. Ed.*, **50**, 10453–10456.
97. Geilen, F., vom Stein, T., Engendahl, B., Winterle, S., Liauw, M.A., Klankermayer, J., and Leitner, W. (2011) *Angew. Chem. Int. Ed.*, **50**, 6831–6834.
98. Salas, G., Santini, C.C., Philippot, K., Colliere, V., Chaudret, B., Fenet, B., and Fazzini, P.F. (2011) *Dalton Trans.*, **40**, 4660–4668.
99. Zhu, Y., Kong, Z.N., Stubbs, L.P., Lin, H., Shen, S., Anslyn, E.V., and Maguire, J.A. (2010) *ChemSusChem*, **3**, 67–70.
100. Yan, N., Yuan, Y., Dykeman, R., Kou, Y., and Dyson, P.J. (2010) *Angew. Chem. Int. Ed.*, **49**, 5549–5553.
101. Julis, J., Hölscher, M., and Leitner, W. (2010) *Green Chem.*, **12**, 1634–1639.
102. Rossi, L.M. and Machado, G. (2009) *J. Mol. Catal. A: Chem.*, **298**, 69–73.
103. Jiang, T., Zhou, Y., Liang, S., Liu, H., and Han, B. (2009) *Green Chem.*, **11**, 1000–1006.
104. Kantam, M.L., Reddy, R.S., Pal, U., Sreedhar, B., and Bhargava, S. (2008) *Adv. Synth. Catal.*, **350**, 2231–2235.
105. Yinghuai, Z., Widjaja, E., Pei Sia, S.L., Zhan, W., Carpenter, K., Maguire, J.A., Hosmane, N.S., and Hawthorne, M.F. (2007) *J. Am. Chem. Soc.*, **129**, 6507–6512.
106. Yan, N., Zhao, C., Luo, C., Dyson, P.J., Liu, H., and Kou, Y. (2006) *J. Am. Chem. Soc.*, **128**, 8714–8715.
107. Miao, S., Liu, Z., Han, B., Huang, J., Sun, Z., Zhang, J., and Jiang, T. (2006) *Angew. Chem. Int. Ed.*, **45**, 266–269.
108. Xue, X., Lu, T., Liu, C., Xu, W., Su, Y., Lv, Y., and Xing, W. (2005) *Electrochim. Acta*, **50**, 3470–3478.
109. Huang, J., Jiang, T., Han, B., Wu, W., Liu, Z., Xie, Z., and Zhang, J. (2005) *Catal. Lett.*, **103**, 59–62.
110. Rossi, L.M., Machado, G., Fichtner, P.F., Teixeira, S.R., and Dupont, J. (2004) *Catal. Lett.*, **92**, 149–155.